RESEARCH ACTIVITIES

Research Center of Integrative Molecular Systems

The mission of CIMoS is to analyze molecular systems in nature to find the logic behind the sharing and control of information between the different spatiotemporal hierarchies, with the ultimate goal of creating novel molecular systems on the basis of these findings.

Molecular Origin of 24 Hour Period in Cyanobacterial Protein Clock

Research Center of Integrative Molecular Systems
Division of Trans-Hierarchical Molecular Systems

AKIYAMA, Shuji
Professor

MUKAIYAMA, Atsushi
Assistant Professor

ABE, Jun	Post-Doctoral Fellow	SHINTANI, Atsuko	Technical Fellow
HIYAMA, Takuya	Post-Doctoral Fellow	SUZUKI, Hiroko	Secretary
FUNAKI, Yukino	Technical Fellow		

Circadian (approximately 24 h) clocks are endogenous time-keeping systems encapsulated in living cells, enabling organisms to adapt to daily fluctuation of exogenous environments on the Earth. These time-keeping systems, found ubiquitously from prokaryotes to eukaryotes, share the three characteristics. First, the circadian rhythmicity of the clocks persists even without any external cues (self-sustainability). Second, the period is little dependent on ambient temperature (temperature compensation). Third, the phase of the clock can be reset by external stimuli such as lightning, humidity, or temperature so as to be synchronized to the external phase (synchronization).

KaiC, a core protein of the circadian clock in cyanobacteria, undergoes rhythmic structural changes over approximately 24 h in the presence of KaiA and KaiB (Kai oscillator). This slow dynamics spanning a wide range of both temporal and spatial scales is not well understood, and is central to a fundamental question: What determines the temperature-compensated 24 h period?[1,2] The Kai oscillator reconstitutable *in vitro* is advantageous for studying its dynamic structure through a complementary usage of both X-ray crystallography and solution scattering, its transient response by using physicochemical techniques, and its molecular motion through a collaborative work with computational groups.

Our mission is to explore the frontier in molecular science of the cyanobacterial circadian clock from many perspectives. This Annual Report summarizes our recent activities.

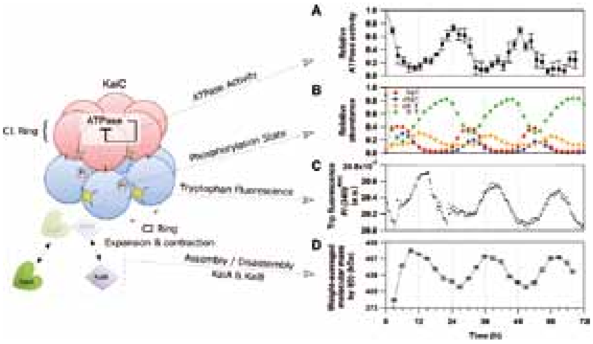

Figure 1. Circadian dynamics of cyanobacterial clock protein KaiC. The C1 and C2 domains in each protomer of KaiC are drawn as red and blue spheres, respectively. Expansion and contraction motions of the C2 ring (B, C) in solution serves as a timing cue for assembly/disassembly of KaiA and KaiB (D), and is interlocked with its C1 ATPase udder a control of negative-feedback regulation (A).

1. Tracking the Ticking of Cyanobacterial Clock Protein KaiC in Solution[3)]

The ATPase activity of KaiC *alone* is strongly correlated with the oscillatory period of the Kai oscillator. This correlation suggests that the ATPase activity of KaiC is one of the period-determining factors of the Kai oscillator. Hence, the determination of the structural change of KaiC interlocked with the ATPase activity is of great of importance.

To track the dynamic transition of KaiC in real-time, we recorded the time evolution of intrinsic tryptophan (Trp) fluorescence from KaiC contained in the Kai oscillator. KaiC is a dumbbell-shaped molecule composed of tandemly duplicated N-terminal (C1) and C-terminal (C2) domains. Six protomers are assembled into a hexamer to attain a double-doughnut shape. Two tryptophan (Trp) residues located in the protomer-protomer interface of the C2 domain can serve as a sensitive probe to monitor the potential structural transition of the C2 ring. The intensity of the Trp fluorescence from KaiC revealed a rhythmic fluctuation with the period of approximately 24 h (Figure 1, panel C). So far as we know, this is the first experimental evidence that demonstrated a dynamic structural transition of the C2 ring of KaiC in solution.

Concomitantly with the Trp-fluorescence dynamics, KaiC underwent a periodic change in its phosphorylation state (Figure 1, panel B). KaiC has the two phosphorylation sites, *i.e.*, Ser431 and Thr432, in the C2 domain, and both residues are phosphorylated and then dephosphorylated in a programmed sequence during the phosphorylation cycle as follows: KaiCS/pT → KaiCpS/pT → KaiCpS/T → KaiCS/T (where ‘S’ represents Ser431, ‘pS’ represents phosphorylated Ser431, ‘T’ represents Thr432, and ‘pT’ represents phosphorylated Thr432). Interestingly, the Trp fluorescence was maximized at the timing when the KaiCpS/T state was populated (Figure 1, panels B and C). The result suggests the Trp fluorescence is an excellent measure of the phosphor-coupled transition of the C2 ring in KaiC.

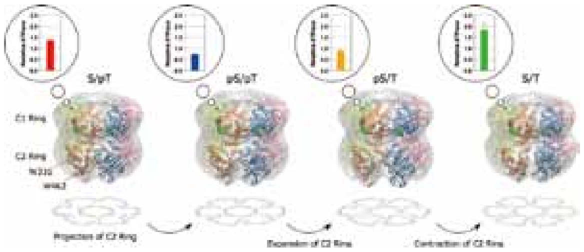

Figure 2. Expansion and contraction motions of C2 ring of KaiC interlocked with ATPase activity.

2. Visualization of Dynamic Structural Changes of KaiC Using Small-Angle X-Ray Solution Scattering Technique[3,4]

To visualize the C2-ring dynamics confirmed by tracking Trp fluorescence, we measured the small-angle x-ray scattering (SAXS) from KaiC in solution. To obtain the SAXS data of biological samples in solution, one must first record the scattering intensity of the sample (biomacromolecules in solution) and then that of the matching buffer in the separate experiment, and finally find the difference between two intensities. The cuvette used for conventional SAXS experiments has only a single observation chamber in order to ensure the qualitative subtraction of the scattering contributed by the solvent molecules. On the other hand, the use of the single-chamber cuvette makes both the experiment and analysis time-consuming.

To record the SAXS pattern of KaiC both efficiently and qualitatively, we designed and constructed an eight-chamber cuvette (octuplet cuvette), each chamber of which was fabricated so uniformly to ensure the inter-chamber subtraction. The developed cuvette enabled us to acquire SAXS dataset of KaiC roughly 10 times faster without any significant degradation of data quality.

On the basis of the obtained SAXS data, we built low-resolution models of the KaiC hexamer as shown in Figure 2. The overall shape is almost unchanged in the transition from KaiCS/pT to KaiCpS/pT, whereas the radius of the C2 ring is dramatically enlarged in the subsequent transition from KaiCpS/pT to KaiCpS/T. The expanded C2 ring is partly contracted in the transition from KaiCpS/T to KaiCS/T, and is further contracted in the subsequent transition from KaiCS/T to KaiCS/pT. The present model suggests that KaiC ticks through expanding and contracting motions of the C2 ring.

The dynamic motion of the C2 ring uncovered throughout our study is chronobiologically meaningful, we believe, in terms of the elucidation of the key conformational change tightly coupled to the period-determining ATPase of KaiC. Our group is trying to improve spatio-temporal resolution of the experiments so as to draw a more dynamic and detailed picture of KaiC ATPase.

3. Instrumentation for the Molecular Origin of 24 Hour Period in Cyanobacterial Circadian Clock

How can biological-clock systems be so slow and stable? It is important to revisit the biological and structural backgrounds for the slowness and specificity both experimentally and theoretically. For this purpose, much effort has been focused on designing dedicated instrumentations for the molecular origin of the circadian period. We have made considerable improvements of instrument stability, signal-to-noise ratio, time resolution, temperature control, automated high-throughput measurements each for fluorescence tracking system,[3] auto-sampling device (unpublished work), HPLC (unpublished work), FTIR (unpublished work) and so on. Using the developed device, we recently succeeded in site-specific monitoring of conformational change of KaiC in solution, and also in identifying a core process of generating circadian periodicity in cyanobacterial circadian clock.[5]

References

1) S. Akiyama, *Cell. Mol. Life Sci.* **69**, 2147–2160 (2012).

2) A. Mukaiyama, T. Kondo and S. Akiyama, *SPring-8 Research Frontiers 2011* 47–48 (2012).

3) Y. Murayama, A. Mukaiyama, K. Imai, Y. Onoue, A. Tsunoda, A. Nohara, T. Ishida, Y. Maéda, T. Kondo and S. Akiyama, *EMBO J.* **30**, 68–78 (2011).

4) S. Akiyama and T. Hikima, *J. Appl. Crystallogr.* **44**, 1294–1296 (2011).

5) Y. Mukaiyama, M. Osako, T. Hikima, T. Kondo and S. Akiyama, submitted.

Theoretical Studies of Chemical Dynamics in Condensed and Biomolecular Systems

Research Center of Integrative Molecular Systems
Division of Trans-Hierarchical Molecular Systems

ISHIZAKI, Akihito
Research Associate Professor

YAMADA, Mariko Secretary

Photosynthesis provides the energy source for essentially all living things on Earth, and its functionality has been one of the most fascinating mysteries of life. Photosynthetic conversion of the energy of sunlight into its chemical form suitable for cellular processes involves a variety of physicochemical mechanisms. The conversion starts with the absorption of a photon of sunlight by one of the light-harvesting pigments, followed by transfer of electronic excitation energy to the reaction center, where charge separation is initiated. At low light intensities, surprisingly, the quantum efficiency of the transfer is near unity. A longstanding question in photosynthesis has been the following: *How does light harvesting deliver such high efficiency in the presence of disordered and fluctuating dissipative environments?* At high light intensities, on the other hand, the reaction center is protected by regulation mechanisms that lead to quenching of excess excitation energy in light harvesting proteins. The precise mechanisms of these initial steps of photosynthesis are not yet fully elucidated from the standpoint of molecular science.

1. An Analytical Continuation Approach for Evaluating Emission Lineshapes of Molecular Aggregates and the Adequacy of Multichromophoric Förster Theory

In large photosynthetic chromophore-protein complexes not all chromophores are coupled strongly, and thus the situation is well described by formation of delocalized states in certain domains of strongly coupled chromophores. In order to describe excitation energy transfer among different domains without performing extensive numerical calculations, one of the most popular techniques is a generalization of Förster theory to multichromophoric aggregates (generalized Förster theory) proposed by Sumi [*J. Phys. Chem. B* **103**, 252 (1999)] and Scholes and Fleming [*J. Phys. Chem. B* **104**, 1854 (2000)].

The aim of this project is twofold. In the first place, by means of analytic continuation and a time convolutionless quantum master equation approach, a theory of emission lineshape of multichromophoric systems or molecular aggregates was proposed.1) In the second place, a comprehensive framework that allows for a clear, compact and effective study of the multichromophoric approach in the full general version proposed by Jang, Newton and Silbey [*Phys. Rev. Lett.* **92**, 218301 (2004)] was developed.1)

We applied the present theory to simple paradigmatic systems and we showed on one hand the effectiveness of time-convolutionless techniques in deriving lineshape operators and on the other hand we showed how the multichromophoric approach can give significant improvements in the determination of energy transfer rates in particular when the systems under study are not the purely Förster regime. The presented scheme allows for an effective implementation of the multichromophoric Förster approach which may be of use for simulating energy transfer dynamics in large photosynthetic aggregates, for which massive computational resources are usually required. Furthermore, our method allows for a systematic comparison of multichromophoric Förster and generalized Förster theories and for a clear understanding of their respective limits of validity.

2. Interactions between Quantum Mixing and the Environmental Dynamics Controlling Ultrafast Photoinduced Electron Transfer Reaction

All the photosynthetic reaction centers (RCs) share considerable similarities in the nature and arrangement of the redox cofactors. The primary charge separation in photosystem II (PSII) of green plants was assumed to be similar to purple bacteria. In the mid-1990s, the charge separation in the PSII RC was shown to follow a different mechanism than bacterial RCs. In the 2000s, the primary charge separation in the PSII RC was investigated by independent studies using femtosecond pump-probe spectra of the D1/D2/cyt*b*559 complex isolated from PSII in the visible/mid-IR [Groot, *et al.*, *Proc. Natl. Acad. Sci. USA* **102**, 13087 (2005).] and visible [Holzwarth, *et al.*, *Proc. Natl. Acad. Sci. USA* **132**, 6895 (2006).] spectral regions. Both reports identified the accessory chlorophyll as the primary electron donor and pheophytin as the primary electron acceptor. Time constants of 600–800 fs and 3 ps were extracted for the pheophytin reduction, which yielded values of 200–300 fs and 1 ps as the intrinsic time constant of the primary charge separation. Theoretical analyses of time-dependent emissions from the PSII core complex yielded 100 fs as the intrinsic time constant. [Raszewski and Renger, *J. Am. Chem. Soc.* **130**, 4431 (2008).] Regardless of the controversial differences, all the values for the PSII RC are faster than the time constant of 3 ps measured for the primary electron transfer (ET) starting from the special pair in purple bacterial RCs. An ultrafast primary charge separation pathway was also revealed in a purple bacterial RC (approximately 400 fs), which starts from the accessory bacteriochlorophyll. [van Brederode, *et al.*, *Biochemistry* **36**, 6855 (1997).] The coupling strengths between electron donors and acceptors are usually thought to be tens of cm^{-1}, and the precise mechanisms enabling the subpicosecond charge separation are mostly unknown.

The timescales of most environmental dynamics, such as solvation or protein reorganization involved in photoinduced ET, occur in the subpicosecond and picosecond range. Thus, the reported subpicosecond timescales imply that the ET reaction may take place beyond the nonadiabatic limit; an adiabatic fashion in which the reaction is dominated by vibrational/environmental motions in an adiabatic (free) energy surface that reflects quantum mixing between the initial and final states.

In this project, to explore the potential causes for subpicosecond timescales of the primary charge separation in photosynthetic RCs, we investigated the interactions between environmental dynamics and quantum mixing that affects the ultrafast photoinduced ET dynamics using quantum dynamics simulation. It was shown that the timescales of environmental dynamics change the nature of the ET reaction (*i.e.*, adiabatic or nonadiabatic), dramatically affect the rates and temperature dependences, and enable subpicosecond reactions despite small donor–acceptor coupling.2)

References

1) L. Banchi, G. Costagliola, A. Ishizaki and P. Giorda, *J. Chem. Phys.* **138**, 184107 (14 pages) (2013).

2) A. Ishizaki, *Chem. Lett.* **42**, 1406–1408 (2013).

Ultimate Quantum Measurements for Quantum Dynamics

Research Center of Integrative Molecular Systems
Division of Trans-Hierarchical Molecular Systems

SHIKANO, Yutaka
Research Associate Professor

HARDAL, Ali Umit Cemal	Visiting Scientist*
NAKANE, Junko	Secretary

Due to great development on experimental technologies, it is possible to capture quantum dynamics in some physical and chemical systems. On the other hand, all experiments are in principle open and dissipative systems. Up to now, the well-explained experiments are approximated to the equilibrium situation. However, by recent technological development, some experiments reach to a transition from equilibrium to non-equilibrium situations. While there are the well-known tools on the non-equilibrium situations; the linear response theory and the Keldysh Green function method, this analysis cannot basically catch dynamical situations. Our goal is to construct the time-resolved theoretical models included the non-equilibrium situations. However, the quantum measurement theory is needed on measuring quantum dynamics, especially considering the measurement backaction. Our current activities are to resolve how sensitive (quantum) measurement can we carry out in principle, to build up some toy models on quantum dynamic, and to explain photoluminescence phenomena in nitrogen vacancy center in diamond and in the semiconductor microcavity.

1. Quantum Measurement Sensitivity without Squeezing Technique[1–4]

As alluded before, our aim is to capture quantum dynamical phenomena. Capturing some phenomena needs to carry out the measurement. The conventional quantum measurement technique has huge measurement backaction. The measurement backaction prevents us chasing quantum dynamics like the classical trajectory. On the other hand, reducing the measurement backaction needs the tiny coupling between the target and probe quantum systems. However, under this situation, the signal in the probe system is also tiny small, that is, it is difficult to capture information. To resolve this problem, the squeezing technique was proposed and was experimentally implemented. However, this technique is practically difficult to be implemented. Our proposal is to use the weak measurement initiated by Aharonov, Albert, and Vaidman without squeezing technique. The profound meaning and interpretation of the weak measurement is seen in the review paper.[3] The key of this method is to take the post-selection of the target system. Due to this effect, tiny probe signal can be amplified. In the original proposal by Aharonov, Albert, and Vaidman, the amplification factor is infinite by the approximation method. However, the effect measurement backaction is simultaneously amplified. When the probe state is Gaussian to be used in the original proposal, we have analytically shown the upper bound of the amplification factor. We have analytically derived the probe state to maximally amplify the signal by the variational method.[1,2] By this optimal probe state, the amplification factor has no upper bound. Our result tells us the infinitely amplified single under the known coupling between the target and the probe. However, in this result, we ignore the physical implementation. As the preliminary result, we demonstrate the single effect for the Laguerre-Gauss modes.3)

2. Discrete Time Quantum Walk as Quantum Dynamical Simulator5–10)

The discrete time quantum walk is defined as a quantum mechanical analogue of the classical random walk but is not the quantization of the classical random walk. This mathematical description is very simple but leads to many quantum dynamical phenomena. This is a toy model to better understand the quantum dynamics. Also, this has recently been various experimental demonstrations in the ultracold atoms in the optical lattice, trapped ions, and optical systems. Recently, we propose the physical implementation in the solid-state system using the nitrogen-vacancy centers in diamond and superconducting qubit.10) We have analytically shown that the one- and two-dimensional discrete time quantum walks can be taken as the quantum dynamical simulator,8) which concept is to emulate some classes of the differential equations, for example, the Dirac equation. Our approximation is used from the discrete lattice to continuous line for the large time steps of the discrete time quantum walk. This mathematical treatment is so powerful like the relationship between the cellular automaton and the integrable system.

3. Photoluminescence Phenomenon from Solid-State System11)

A method to measure some physical properties by light is widely used in physical, chemical, and biological systems. Therefore, laser science has been developed along with our demands from science and technology. A single photon source is expected as the low power laser source and the quantum communication tool. A nitrogen vacancy center in diamond and a quantum dot in a semiconductor system are the promising candidate of the single photon source. Especially, a nitrogen vacancy center in diamond has been attracted since this is run at room temperature. For an application as the highly controlled photon source, the photoluminescence process in the nitrogen vacancy center in diamond needs to be well understood. This system has the $S = 1$ electronic spin with the hyperfine structure 2.87 GHz. Furthermore, inserting a magnetic field, the different magnetic states are separated due to the Zeeman shift. Since this electronic spin is highly localized, the local magnetic field evaluation is needed. We have shown the method to evaluate the local magnetic field from the conventional confocal microscopy. Also, the nitrogen vacancy center in diamond is a candidate of the quantum memory. Since a lifetime of the nuclear spin of a ^{13}C atom nearly located in the nitrogen vacancy spot is long (~ sec order), the perfect quantum state transfer is needed. However, we have proposed the simple spin transfer scheme under the dissipative situation.10) As the next step, we will study the photoluminescence process from the nitrogen vacancy center in diamond.

As the current activities of our group, we are studying the photoluminescence processes of the quantum dots and the exciton-polariton Bose-Einstein condensations in the two dimensional electronic gas of the semiconductor. Experimentally, we measure the photoluminescence by the confocal microscopy. These materials are expected to be used as the classical optical devices; the optical switching, collaborated with the various experimentalists.11)

References

1) Y. Susa, Y. Shikano and A. Hosoya, *Phys. Rev. A* **85**. 052110 (2012).
2) Y. Susa, Y. Shikano and A. Hosoya, *Phys. Rev. A* **87**, 046102 (2013).
3) H. Kobayashi, G. Puentes and Y. Shikano, *Phys. Rev. A* **86**, 053805 (2012).
4) Y. Shikano, *Phys. Scr.* **T151**, 014015 (2012).
5) Y. Shikano, T. Wada and J. Horikawa, *Phys. Scr.* **T151**, 014016 (2012).
6) Y. Shikano, *Quant. Infor. Proc.* **11**, 1013 (2012).
7) Y. Shikano, E. Segawa, A. Perez and J. Wang, *J. Comput. Theor. Nanosci.* **10**, 1555 (2013).
8) Y. Shikano, *J. Comput. Theor. Nanosci.* **10**, 1558 (2013).
9) M. Gonulol, A. Ekrem, Y. Shikano and O. E. Mustecaplioglu, *J. Comput. Theor. Nanosci.* **10**, 1596 (2013).
10) A. U. C. Hardal, P. Xue, Y. Shikano, O. E. Mustecaplioglu and B. C. Sanders, *Phys. Rev. A* **88**, 022303 (2013).
11) T. Horikiri, Y. Matsuo, Y. Shikano, A. Loffler, S. Hofling, A. Forchel and Y. Yamamoto, *J. Phys. Soc. Jpn.* **82**, 084709 (2013).

---

* IMS International Internship Program

Studies of Field-Effect-Transistor Based on Highly-Correlated Molecular Materials

Research Center of Integrative Molecular Systems
Division of Functional Molecular Systems

YAMAMOTO, Hiroshi
Professor

SUDA, Masayuki
Assistant Professor

URUICHI, Mikio
Technical Associate

LE GOFF, Florian	Visiting Scientist*
SHIMIZU, Atsuko	Secretary

Field effect transistors (FETs) with organic channel materials are under intense studies because of the possibilities of application in flexible, printable, and large-area electronic devices. Despite single-component neutral molecules like pentacene and ruburene are mainly investigated to pursuit high performance (*ex.* high mobility *etc.*) organic FETs, few studies are known for FETs based on compound-type organic semiconductors. We have been exploiting FET devices with charge-transfer salts of organic molecules, namely cation-radical salts of electron-donating molecules (donors) such as BEDT-TTF and anion-radical salts of electron accepting molecules (acceptors) such as $Ni(dmit)_2$. Among these materials, our focus concentrates in Mott-insulators in which Coulomb interaction among carriers blocks metallic transport. In this highly correlated situation of charge carriers, Mott insulator stays in a fragile semiconducting state, where carrier injection, chemical and/or physical pressure (or strain), and thermal fluctuation can drive it into a metallic state by phase transition (*i.e.* Mott transition: Figure 1). One can expect an abrupt change of the conductivity of device due to phase transition that is induced by very small external stimuli. More specifically, it is anticipated that the Mott-insulating state can be switched to a metallic state by a field effect, since the carrier density (band-filling) of a FET interface can be finely modulated by an electrostatic field from the gate electrode. Indeed, our previous work showed such an insulator-to-metal transition in terms of the band structure, and these results provide not only a possibility of application use of organic Mott-FET but also a significant insight into the mechanism of Mott transition itself. We are now expanding our research target both to the superconducting transition of Mott-FET and to its room-temperature operation.

(BEDT-TTF = bis(ethylenedithio)tetrathiafulvalene,
dmit = 1,3-dithiole-2-thione-4,5-dithiolate)

1. Field-Induced Superconductivity in an Organic Mott-FET

κ-(BEDT-TTF)$Cu[N(CN)_2]Br$ (κ-Br) is an organic super-

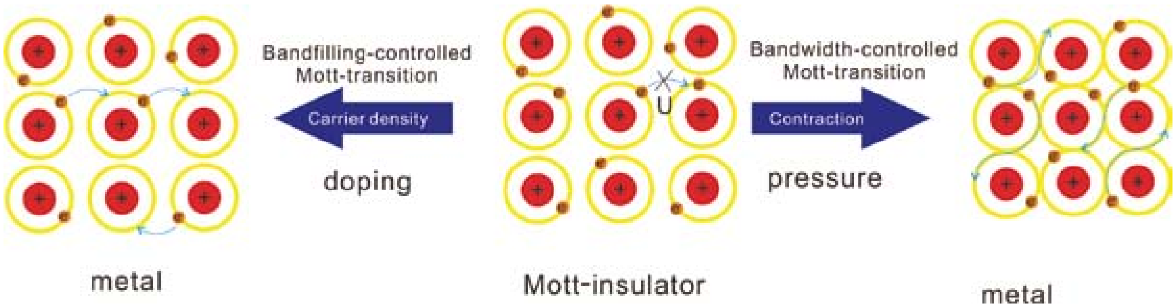

Figure 1. Concept of a Mott-insulator (center) along with its bandfilling-controlled (left) and bandwidth-controlled (right) Mott transitions. When the band is half-filled and band energy is small, the carriers are localized because of on-site Coulomb interaction (*U*). This situation is broken down either by changing the carrier concentration or by compressing the lattice. In many cases, the Mott transitions are associated with superconductivity at the boundary between metallic and insulating phases.

conductor whose electronic state is Mott-insulating at room-temperature but turns into metallic at low temperature through a crossover around 50–100 K, possibly because of an increase of bandwidth upon thermal contraction. In our previous works, a tensile strain altered its ground state into a Mott-insulating state, when its thin (100–300 nm) crystal is laminated on top of SiO_2/Si^{++} substrate and cooled down to low temperature. Although the electronic state at low temperature became completely insulating in this experiment because of the very small thermal expansion coefficient of Si substrate (2 ppm/K), one can anticipate from the *T–P* (temperature *vs.* pressure) phase diagram that mixed electronic state between superconducting and Mott-insulating states can be realized when the tensile strain is much weaker. To achieve such a mixed state (or, percolate-superconducting state) in the device, where phase-separation occurs between superconducting and Mott-insulating states, we have chosen Nb-doped $SrTiO_3$ as a back-gate substrate because of its larger thermal expansion coefficient (*ca.* 10 ppm/K) than Si. An aluminum oxide layer was grown by atomic layer deposition technique to form a gate dielectric on the substrate. After lamination of κ-Br on the substrate, the Mott-FET device which showed a weakly insulating behavior at low temperature was fabricated (Figure 2).

Upon applying a positive gate voltage, the resistivity went down and weakly metallic behavior was observed at $V_G > 2$ V. By further increasing the gate voltage up to 8 V, the device showed a sudden drop of resistivity around 5 K, which can be attributed to superconductivity. Taking into account of bistable I–V characteristics observed in the low resistance region, the above transition can be understood as a percolation transition of superconducting islands that is induced by the electrostatic doping of electrons. The transition temperature increased as the gate voltage rose and saturated around $V_G = 11$ V. The above result is the first example of field-induced superconductivity in organic materials, and can be utilized for uncovering a phase diagram of organic Mott system in the simultaneous control of band filling and band width.$^{1)}$

2. Operation of Organic Mott-FET at Higher Temperature

In order to operate the organic Mott-FET at higher temperature, hopefully at room temperature, it is necessary to realize much larger Mott gap energy and thinner crystal thickness. For this purpose, we are examining several strategies in parallel.

κ-(BEDT-TTF)$Cu[N(CN)_2]Cl$ (κ-Cl) is a Mott-insulator with larger Mott gap than κ-Br and is therefore suitable for examining the influence of an increase in Mott-gap energy on the device performance. For example, it has higher resistance than κ-Br and exhibit better ON/OFF ratio. In addition, it always shows ambipolar behavior, probably because of its clean surface. This situation allows us to analyze the critical exponents of filling-controlled Mott transition, which will give us important information about ON/OFF efficiency of the device (Figure 3).$^{2)}$ Because it is also possible to control the Mott gap energy by applying a mechanical strain, κ-Cl device provides an ideal platform to expand Mott-FET strategy to higher temperature.

Another candidate of the channel material for Mott-FET that can be used at room temperature is (BEDT-TTF)(TCNQ). We are exploiting this material both in a crystalline and amorphous form to find a better FET setup for simple but highly efficient device operatable at room temperature. (TCNQ = tetracyanoquinonedimethane)

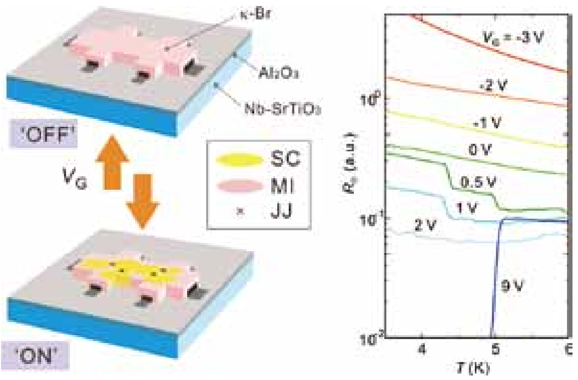

Figure 2. The device structure and temperature dependency of device resistance under various gate voltages. The device comprises κ-Br thin-layer single crystal and $Al_2O_3/SrTiO_3$ substrate. By applying a positive gate voltage, the resistance of the device starts decreasing, while a negative gate voltage results in an increase of the resistance. Although superconducting (SC) and Mott-insulating (MI) phases are separated in the device, the four-terminal resistance drops to zero when the Josephson junction (JJ) network forms a pathway to shunt the voltage terminals. This kind of percolation transition is clearly observed in the right panel, where the resistance drops at 5 K with a gate voltage of 9 V.

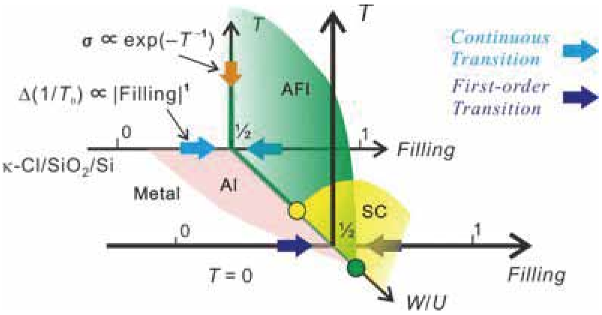

Figure 3. Universal phase diagram based on the experimental results obtained by organic Mott-FETs.

References

1) H. M. Yamamoto, M. Nakano, M. Suda, Y. Iwasa, M. Kawasaki and R. Kato, *Nat. Commun.* **4**, 2379 (7 pages) (2013).
2) H. M. Yamamoto, J. Ueno and R. Kato, E*ur. Phys. J. Special Topics* **222**, 1057–1063 (2013).

---

* IMS International Internship Program

Synthetic Inorganic and Organometallic Chemistry of Transition Metals

Research Center of Integrative Molecular Systems
Division of Functional Molecular Systems

MURAHASHI, Tetsuro
Professor

YAMAMOTO, Koji
Assistant Professor

HORIUCHI, Shinnosuke	IMS Fellow
KHOURY ATHIEH, Bruno	Visiting Scientist*
TACHIBANA, Yuki	Graduate Student†
KIMURA, Seita	Graduate Student†
ISHIKAWA, Yuki	Graduate Student‡
MASAI, Kohei	Graduate Student
KAWAMATA, Shiori	Research Fellow
TANIWAKE, Mayuko	Secretary
NOGAWA, Kyoko	Secretary

Our research focuses on synthesis and structural elucidation of a new class of transition metal complexes. This research leads to development of fundamental concepts of transition metal chemistry as well as applications to catalysis and materials science. Novel synthetic methods are developed to realize transition metal complexes having unique bonding nature. The newly synthesized transition metal complexes are further converted to more reactive forms, and their reaction mechanisms are elucidated. The aspects gained by this research are applied to the understanding and development of molecular catalysis. Furthermore, unique properties of low-dimensional metal-organic hybrid molecules are investigated and developed in our group.

1. Chemistry of Multinuclear Sandwich Complexes

The molecular sandwich framework is one of the fundamental structures in transition metal chemistry. It had been believed that the structural concept can be applied only to mono- and dinuclear complexes. Our group revealed that the multinuclear sandwich complexes containing a one-dimensional metal chain or a two-dimensional metal sheet exist stably.[1,2] These findings expand the scope of the structural concept of sandwich compounds (Figure 1).

For the two-dimensional metal sheet sandwich complexes, our group has shown that six-, seven-, eight-, and nine-membered carbocycles, as well as polycyclic arenes behave as the excellent binders for metal sheets. These metal sheet sandwich complexes are stable even in solution. Thus, a reactive form of such metal sheet sandwich complexes may provide a new opportunity to develop sandwich type late transition metal catalysts.

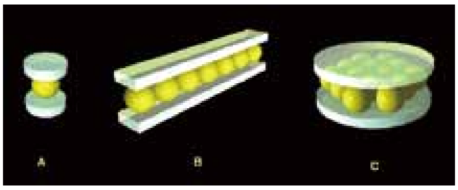

Figure 1. Schematic representation of sandwich compounds: (**A**) mononuclear metallocenes, (**B**) one-dimensional metal chain sandwich complexes, (**C**) two-dimensional metal sheet sandwich complexes. Our group revealed the existence of categories **B** and **C**.

Conversion of Trinuclear Sandwich Complexes to Trinuclear Half-Sandwich Complexes[5)]

Our group recently showed that triangular trimetal sandwich complexes are isolable. It is now known that a variety of cyclic unsaturated hydrocarbons such as arene, cycloheptatrienyl, cycloheptatriene, and cyclooctatetraene work as excellent μ_3-face-capping binder for a Pd_3 moiety.[2–4)] We found that the tripalladium sandwich complexes of [2.2]paracyclophane, cycloheptatriene, and cyclooctatetraene can be converted to trinuclear half-sandwich complexes upon treatment with 1,10-phenanthroline (phen). During the reaction, one of the facially-capping ligands is replaced with three phen ligands. Interestingly, the Pd_3 moiety underwent trinuclear addition to the remaining carbocyclic ligand to form unusual coordination modes. For the [2.2]paracyclophane ligand, a $Pd^0 \rightarrow Pd^{II}$ dative bonded moiety and a Pd^{II} moiety coordinated to an arene ring synfacially in a η^3:η^3 manner (eq. 1). The cycloheptatriene ligand was added by a Pd_3 moiety, where a Pd^I–Pd^I moiety and a Pd^{II} moiety is bound synfacially to the triene face (eq. 2). On the other hand, the Pd_3 moiety added to a cyclooctatetraene to form a cyclooctatetraenetetrayl tripalladium complex, where formally tetraanionic cyclooctatetraene ligand coordinates to three Pd^{II} centers through a $\mu_3:\eta^1:\eta^3:\eta^1:\eta^3$ coordination mode (eq. 3). The tripalladium addition product of cyclooctatetraene further converted to a dihydropentalenediyl complex via intramolecular reductive C–C coupling (eq. 4).

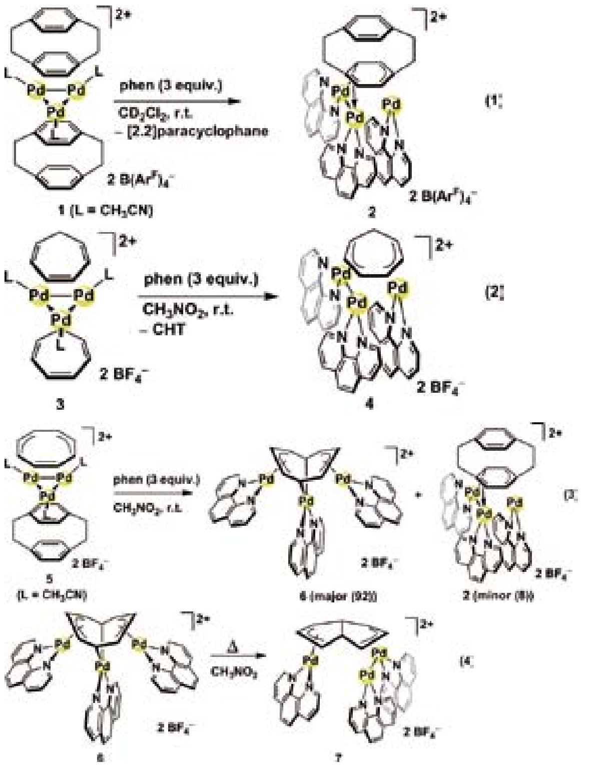

2. Reaction Mechanism of Highly Reactive Pd–Pd Complexes

Our group has shown that a homoleptic dinuclear Pd–Pd complexes of nitriles such as $[Pd_2(CH_3CN)_6][BF_4]_2$ are isolable.[6] These homoleptic solvento-Pd$_2$ complexes are highly substitutionally labile, and allow us to investigate reaction mechanism of the Pd–Pd complexes in details. For example, our group has shown that a Pd–Pd moiety adds to various unsaturated hydrocarbons including arenes in a syn addition manner.[7]

π-Coordination Pyrrole and Indole on a Pd–Pd Bond[8]

We found that pyrrole and indole form stable π-complexes. Thus, the reaction of $[Pd_2(CH_3CN)_6][BF_4]_2$ with pyrrole or indole gave the dinuclear sandwich complexes (eqs 5 and 6). These results provided the first evidence of the π-coordination of azoles having no chelating functionality to a Pd center. Particularly interesting is the coordination mode of indole which used its six-membered ring in the μ-$\eta^2:\eta^2$-coordination. Usually, the carbons at 2- and 3-positions are reactive sites in indole transformations. The bridging coordination mode of indole using six-membered ring carbons at 4-, 5-, 6-, and 7-positions is understood by a qualitative MO consideration: The π-orbital array at 4-, 5-, 6-, and 7-positions is isolobal with that of the 1,3-butadiene, which becomes an excellent bridging ligand on a Pd–Pd bond due to the efficient orbital overlap of diene-type HOMO or LUMO with (dσ–dσ)* or (dσ–dσ).

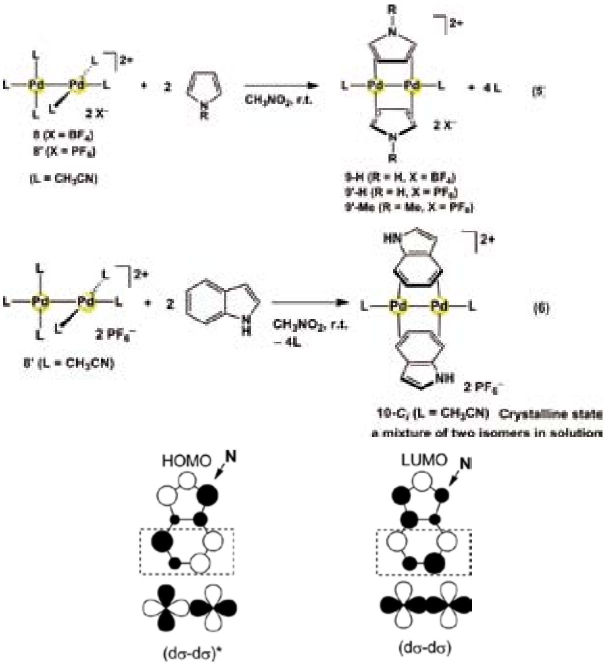

Scheme 1. Schematic representation of the HOMO and the LUMO of indole, and (dσ–dσ)* and (dσ–dσ) of a Pd−Pd moiety.

References

1) For the first report on the metal chain sandwich complexes: T. Murahashi, *et al.*, *J. Am. Chem. Soc.* **121**, 10660–10661 (1999).
2) For the first report on the metal sheet sandwich complexes: T. Murahashi, *et al.*, *Science* **313**, 1104–1107 (2006).
3) T. Murahashi *et al.*, *Angew. Chem., Int. Ed.* **46**, 5440–5443 (2007).
4) T. Murahashi *et al.*, *J. Am. Chem. Soc.* **130**, 8586–8587 (2008).
5) T. Murahashi, K. Takase, K. Usui, S. Kimura, M. Fujimoto, T. Uemura, S. Ogoshi and K. Yamamoto, *Dalton Trans.* **42**, 10626–10632 (2013).
6) (a) T. Murahashi, *et al.*, *Chem. Commun.* 1689–1690 (2000). (b) T. Murahashi *et al.*, *J. Am. Chem. Soc.* **128**, 4377–4388 (2006).
7) T. Murahashi *et al.*, *J. Am. Chem. Soc.* **133**, 14908–14911 (2011).
8) T. Murahashi, S. Kimura, K. Takase, S. Ogoshi and K. Yamamoto, *Chem. Commun.* **49**, 4310–4312 (2013). This paper was published in the special issue “Emerging Investigators 2013.”

* IMS International Internship Program

† carrying out graduate research on Cooperative Education Program of IMS with Osaka University

‡ carrying out graduate research on Cooperative Education Program of IMS with Rikkyo University

Development of Organic Semiconductors for Molecular Thin-Film Devices

Research Center of Integrative Molecular Systems
Division of Functional Molecular Systems

SUZUKI, Toshiyasu
Associate Professor

SAKAMOTO, Youichi
Assistant Professor

KURODA, Yasuhiro Post-Doctoral Fellow
WATANABE, Yoko Secretary

Organic light-emitting diodes (OLEDs) and organic field-effect transistors (OFETs) based on π-conjugated oligomers have been extensively studied as molecular thin-film devices. Organic semiconductors with low injection barriers and high mobilities are required for highly efficient OLEDs and OFETs. Radical cations or anions of an organic semiconductor have to be generated easily at the interface with an electrode (or a dielectric), and holes or electrons must move fast in the semiconducting layer. Compared with organic p-type semiconductors, organic n-type semiconductors for practical use are few and rather difficult to develop. We found that perfluorinated aromatic compounds are efficient n-type semiconductors for OLEDs and OFETs.

1. Optical Properties of Fully and Partially Fluorinated Rubrene in Films and Solution[1)]

We present the optical properties of fully ($C_{42}F_{28}$, **PF-RUB**) and half-fluorinated ($C_{42}F_{14}H_{14}$, **F14–RUB**) rubrene, both in thin films and as monomers in solution and compare them to hydrogenated rubrene ($C_{42}H_{28}$, **RUB**). All three compounds show similar optical absorption bands and photoluminescence line shapes. The results are interpreted with density functional calculations of the orbital energies and time-dependent density functional theory for the HOMO–LUMO transition. Red shifts induced by the surrounding solvent or organic thin films remain much smaller than for polyacenes, in keeping with previous observations for rubrene and existing models for the solvatochromic shifts.

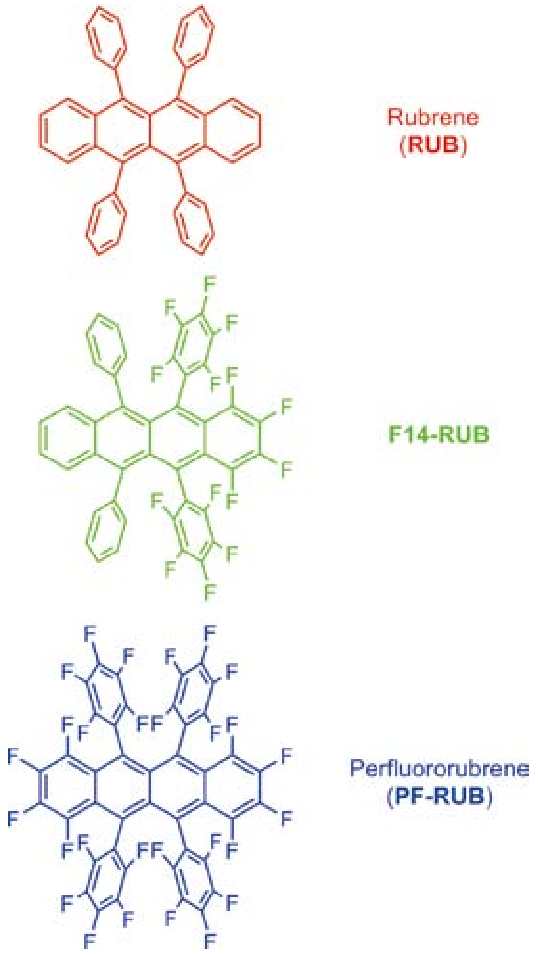

Figure 1. Structures of **RUB**, **F14-RUB**, and **PF-RUB**.

2. Selective Synthesis of [6]-, [8]-, and [10] Cycloparaphenylenes²⁾

The selective synthesis of [6]-, [8]-, and [10]cycloparaphenylenes (CPPs) was achieved by a new synthetic route involving Ni(0)-mediated coupling of bis(*para*-haloaryl)dinuclear arylplatinum complexes and the reductive elimination of the complexes. Importantly, the highly strained [6]CPP was prepared in good overall yield.

3. Experimental Reorganization Energies of Pentacene and Perfluoropentacene: Effects of Perfluorination³⁾

Electron–phonon coupling of the highest occupied molecular orbital (HOMO) state is studied by high-resolution ultraviolet photoelectron spectroscopy (UPS) for pentacene (PEN) and perfluoropentacene (PFP) monolayers on graphite. The reorganization energy and related coupling constants associated with the interaction between holes and molecular vibrations are obtained experimentally using a single mode analysis (SMA) of the observed vibronic-satellite intensities of the monolayers. The results are compared with those estimated by multimode analyses of UPS spectra and those derived by means of theoretical approaches, indicating that the purely experimental method with SMA is useful for studying the reorganization energy and the hopping mobility of organic systems. Furthermore, we found that the reorganization energy of PFP is significantly greater than that of PEN, which is ascribed to the extended HOMO distribution of PFP by perfluorination of PEN. The comparison with the results derived from gas-phase UPS measurements is also discussed.

References

1) F. Anger, R. Scholz, E. Adamski, K. Broch, A. Gerlach, Y. Sakamoto, T. Suzuki and F. Schreiber, *Appl. Phys. Lett.* **102**, 013308 (2013).

2) E. Kayahara, T. Iwamoto, T. Suzuki and S. Yamago, *Chem. Lett.* **42**, 621–623 (2013).

3) S. Kera, S. Hosoumi, K. Sato, H. Fukagawa, S. Nagamatsu, Y. Sakamoto, T. Suzuki, H. Huang, W. Chen, A. T. S. Wee, V. Coropceanu and N. Ueno, *J. Phys. Chem. C* **117**, 22428–22437 (2013).

Building Photosynthesis by Artificial Molecules

Research Center of Integrative Molecular Systems
Division of Functional Molecular Systems

NAGATA, Toshi
Associate Professor (–March, 2013)*

SAKURAI, Rie	IMS Fellow	WANATABE, Yoko	Secretary
YUSA, Masaaki	Graduate Student		
MIURA, Takahiro	Technical Fellow		

The purpose of this project is to build nanomolecular machinery for photosynthesis by use of artificial molecules. The world's most successful molecular machinery for photosynthesis is that of green plants—the two photosystems and related protein complexes. These are composed almost exclusively from organic molecules, plus a small amount of metal elements playing important roles. Inspired by these natural systems, we are trying to build up multimolecular systems that are capable of light-to-chemical energy conversion. At present, our interest is mainly focused on constructing necessary molecular parts and examining their redox and photochemical behavior.

1. Synthesis and Dynamic Behavior of Tweezer-Like Molecules with Opposite Electric Charges

The biological photosynthetic devices have mostly static structures that are optimized for efficient energy transfer and charge separation. After the photoinduced charge separation, however, many chemical transformations are necessary to complete the light-to-chemical energy conversion. For this particular purpose, it is rather beneficial to introduce "dynamic" structural features, because chemical transformation is often accompanied by substantial structural change of the substrates.

We aimed at introducing dynamic behavior on photosynthetic model compounds. The ultimate goal should be control of chemical transformation by way of photoinduced electron transfer. Presently, we focus on the synthesis of molecules that potentially respond to local electric field resulting in structural change.

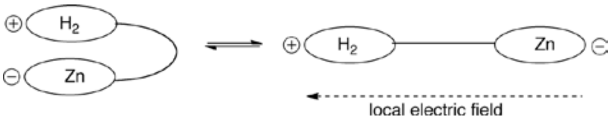

Figure 1. The design of the tweezer molecule.

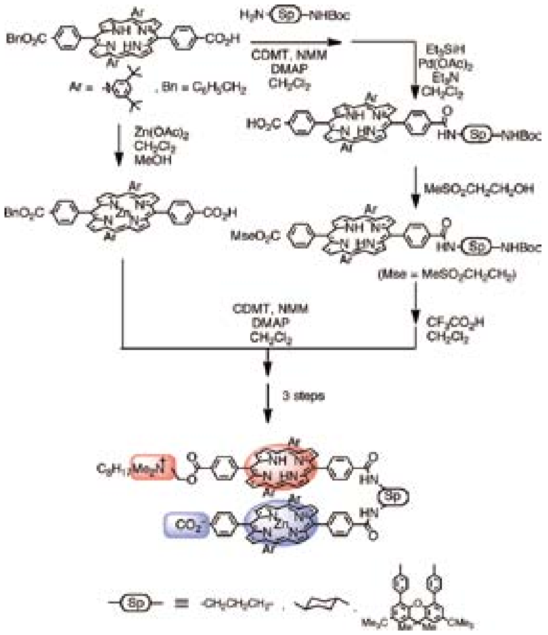

Figure 2. Synthesis of the tweezer molecule.

The design of the target molecule is shown in Figure 1. The molecule has a tweezer-like structure, with a free-base porphyrin and a zinc porphyrin at both ends. The shape of the

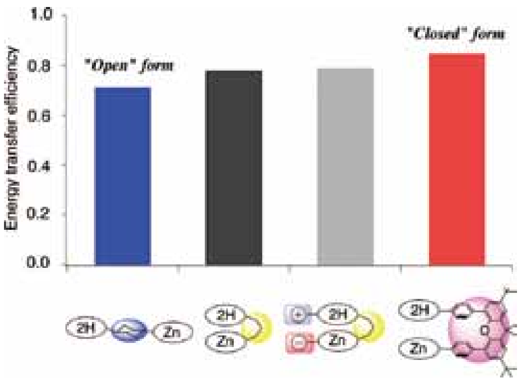

Figure 3. The fluorescence energy transfer efficiencies for the tweezer molecules and reference molecules.

molecule can be estimated from the degree of the fluorescence energy transfer from the zinc porphyrin to the free-base porphyrin. Moreover, there are introduced two opposite charges on both ends.

The synthesis of the tweezer molecule is shown in Figure 2. Three different spacers were used: Trimethylene (flexible), cyclohexane-1,4-diyl (fixed at "open" conformation), and xanthene-1,8-diyl (fixed at "closed" conformation). The equilibrium conformations of these molecules were estimated by fluorescence energy transfer experiments (Figure 3). The trimethylene-bridged molecules were found to have intermediate conformation between "open" and "closed" forms. Contrary to our expectation, the conformations of the tweezer molecules did not change when two opposite charges were introduced at both ends. In fact, molecular dynamic simulations revealed that the aryl substituents on the porphyrin rings caused substantial steric repulsion that precludes approach of the two charges at the ends. Simulations also revealed that if the charges were introduced at the 10-positions (instead of the 15-position as in the present molecules), the charges can approach each other in spite of the steric repulsion of the aryl substituents.

2. Synthesis of a Ternary Binucleating Ligand with 1,2,4-Triazole Bridge and Its Metal Complexes

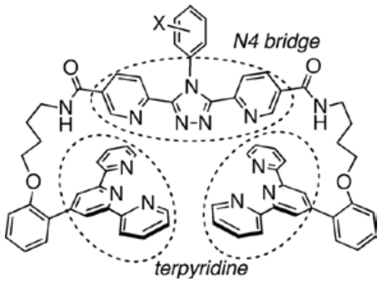

Figure 4. The new ternary binucleating ligand with 1,2,4-triazole bridge.

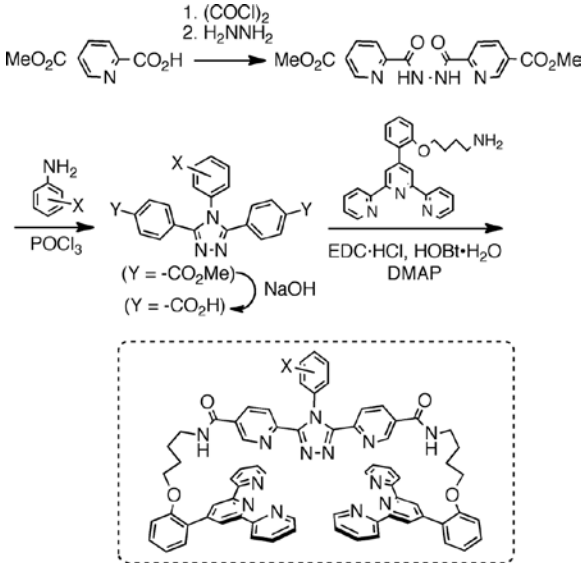

Figure 5. Synthesis of the ternary binucleating ligand.

Multinuclear transition metal complexes are promising components for artificial photosynthesis, because of their ability to perform multielectron redox reactions. One challenging issue is to use 3d transition metals for this purpose. The 4d and 5d transition metals (Ru and Ir in particular) are frequently used in the area of artificial photosynthesis, however they are expensive and better to be replaced with cheaper 3d metals. Our group have been tackling this problem by use of multidentate organic ligands.[1–3] Herein we report the synthesis of new "ternary" binucleating ligands consisting of two terpyridines and one "N4 bridge," 3,5-bis(2-pyridyl)-1,2,4-triazole (Figure 4).

Synthesis of the ligand is shown in Figure 5. Treatment of the ligand with $Co(OAc)_2$ and $Ni(OAc)_2$ afforded metal complexes with formula $[LM_2(OAc)]^{3+}$ (L = ligand, M = Co or Ni). Unlike the ternary binucleating ligands with phthalazine-containing N4 bridges (which we previously reported,[3]) complexes with μ_2, η^1-bridging anions (like OH^- or Cl^-) were not observed. Such difference can be ascribed to the presence of the 5-membered ring in the present ligand, which causes larger metal-to-metal distances in comparison with the 6-membered ring in the phthalazine system. This reasoning was also supported by the preliminary X-ray results of the $[LCo_2(OAc)]^{3+}$ complex.

References

1) H. Kon and T. Nagata, *Inorg. Chem.* **48**, 8593–8602 (2009).
2) H. Kon and T. Nagata, *Chem. –Eur. J.* **18**, 1781–1788 (2012).
3) H. Kon and T. Nagata, *Dalton Trans.* **42**, 5697–5705 (2013).

---

* Present Position; Professor, Department of Applied Chemistry, Faculty of Science and Technology, Meijo University. Address: 1-501 Shiogamaguchi, Tenpaku, Nagoya 468-8502, Japan

Chemistry of Bowl-Shaped Aromatic Compounds and Metal Nanocluster Catalysts

Research Center of Integrative Molecular Systems
Division of Functional Molecular Systems

SAKURAI, Hidehiro
Associate Professor

HIGASHIBAYASHI, Shuhei
Assistant Professor

SUGIISHI, Tsuyuka	IMS Fellow
MORITA, Yuki	Post-Doctoral Fellow
KUMAR, Selva	Post-Doctoral Fellow
PANDIT, Palash	Post-Doctoral Fellow
MAITY, Prasenjit	Post-Doctoral Fellow
DHITAL, Raghu Nath	Post-Doctoral Fellow
KAMONSATIKUL, Choavarit	Visiting Scientist
JINASAN, Atchaleeya	Visiting Scientist
TSAI, I-Chang	Visiting Scientist
MANNA, Sudipta Kumar	Visiting Scientist
PONGPIPATT, Paweena	Visiting Scientist
SINGH, Priyanka	Visiting Scientist
AGRAWAL, Meghdeep	Visiting Scientist
THONGPAEN, Jompol	Visiting Scientist
ONOGI, Satoru	Graduate Student
KAEWMATI, Patcharin	Graduate Student
KARANJIT, Sangita	Graduate Student
SHRESTHA, Binod Babu	Graduate Student
HAESUWANNAKIJ, Setsiri	Graduate Student
OKABE, Yuki	Graduate Student
SASAKI, Tokiyo	Secretary
HAZAMA, Kozue	Secretary

Bowl-shaped π-conjugated compounds including partial structures of the fullerenes, which are called “buckybowls,” are of importance not only as model compounds of fullerenes but also as their own chemical and physical properties. For example, in solution they show the characteristic dynamic behavior such as bowl-to-bowl inversion. On the other hand, they sometimes favor stacking structure in a concave-convex fashion in the solid state, giving excellent electron conductivity. Furthermore, some buckybowls are conceivable to possess the bowl-chirality if the racemization process, as equal as bowl-to-bowl inversion, is slow enough to be isolated. Very few buckybowls has been achieved for preparation mainly due to their strained structure, and no report on the preparation of chiral bowls has appeared. In this project, we develop the rational route to the various buckybowls with perfect chirality control using the organic synthesis approach.

We also investigate to develop novel catalytic properties of metal nanoclusters. We focus on the following projects: Preparation of size-selective gold nanoclusters supported by hydrophilic polymers and its application to aerobic oxidation catalysts: Synthetic application using metal nanocluster catalyst: Development of designer metal nanocluster catalyst using the highly-functionalized protective polymers.

1. Stereoelectronic Effect of Curved Aromatic Structure Favouring the Unexpected *Endo* Conformation of Benzylic Substituted Sumanene[1)]

Since the discovery of fullerene and carbon nanotubes, curved aromatic compounds including bowl-shaped buckybowls have elicited much attention in science and industry. One principal question in these curved aromatic compounds is the difference between the concave face and the convex face. The curvature affects the nature between the two faces, resulting in differences of the through-space and through-bond effects. The latter would appear as a stereoelectronic effect between the curved aromatic structure and a connected functional group. In general, the stereoelectronic effect is reflected in the conformational stability and chemical reactivity of a molecule. Therefore, it is important to understand such conformations or chemical reactivities as a consequence of stereoelectronic effects. The interpretation of the stereoelectronic effect of curved aromatic compounds would lead to understanding the difference in nature between the two faces. However, no example of stereoelectronic effects of curved aromatic compounds have been found and studied to date. We have found a first example of the stereoelectronic effect of a curved aromatic structure, which dominates the *endo/exo*-R conformational stability of benzylic substituted sumanenes (**1**) (Figure 1).

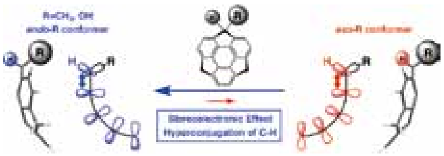

Figure 1. Schematic diagram of the stereoelectronic effect and through-space effects between the bowl and the C-H/C-R of benzylic substituted sumanene.

2. Low-Temperature Carbon–Chlorine Bond Activation by Bimetallic Gold/Palladium Alloy Nanoclusters: An Application to Ullmann Coupling[2)]

In the past decade, nanoclusters (NCs) of bimetallic alloys have attracted considerable research interest because of their unique catalytic properties, which differ substantially from those of single-phase monometallic counterparts. Among the various bimetallic NCs that have been fabricated to date, gold/palladium alloy NCs are particularly fascinating because of their high catalytic activities.

Because of the relatively high dissociation energy of C–Cl bond in comparison with C–Br or C–I, it is difficult to activate chloroarenes by undergoing oxidative addition on Pd without ligation by nucleophilic ligands. Here we demonstrate a new method for activation of C–Cl bonds at low temperature as a result of bimetallic Au/Pd synergy and we report the successful examples of the Ullmann coupling of chloroarenes under ambient conditions. Ullmann coupling, which was first reported in 1901, is a conventional method for the synthesis of symmetrical biaryls. Initially, aryl iodides were used in coupling reactions that were promoted by excess amount of copper at high temperatures. Recent developments in the Ullmann coupling reaction has permitted the use of aryl bromides or chlorides as reactants in the presence of a co-reductant such as Zn powder, formic acid, and dihydrogen under mild conditions. Such reactions can be catalyzed by many types of homogenous or heterogeneous transition-metal catalysts, such as Ni, Pd or Au. However, to the best of our knowledge, there are no reports of any successful examples of Ullmann coupling reactions of chloroarenes under ambient conditions. It is because of relative difficulty in the activation a C–Cl bond, which needs to occur twice within a single catalytic cycle, and because all C–M intermediates need to resist hydrogenation by external co-reductant.

The activity increased markedly for a bimetallic catalyst containing 50% of Pd, giving the coupling product in 98% yield with 100% conversion. The coupling reaction occurred smoothly even when the reaction temperature was decreased to 35 °C or to 27 °C (room temperature) quantitatively for 6 h and 24 h, respectively. To the best of our knowledge, this is the first example of Ullmann coupling of chloroarenes under ambient conditions.

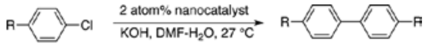

Au:PVP	0%
Pd:PVP	0%
$Au_{0.5}Pd_{0.5}$:PVP	98%

An essential step, which determines the characteristics difference in the catalytic activities of Au, Au/Pd, and Pd NCs is the oxidative addition of chloroarene followed by the spill over of Cl, and we therefore intensively studied only this step at present. Our previous report demonstrated that Au_{20}^-, a negatively charged homogeneous Au NCs, is a suitable model for simulating reaction on the surface of Au:PVP. We therefore examined the model systems Au_{20}^-, $Au_{16}Pd_4^-$, $Au_{10}Pd_{10}^-$, and Pd_{20} to compare the reaction pathway for oxidative additions on Au, Pd, and Au/Pd alloy clusters. Fundamental consideration of these models and the computational details are given in supporting information. The calculations were performed by the Gaussian09 suite of programs. The energy diagram of the oxidative addition of chlorobenzene (**1b**) on Au_{20}^- and $Au_{10}Pd_{10}^-$ is shown in Figure 2 where the energies are shown by taking those of adsorption complexes being the same for these clusters.

In the case of the Au_{20}^- system, **1b** is adsorbed on the facet site and a local minimum is obtained for the dissociative chemisorption (Int_B1). However, the calculated activation energy barrier for this (C–Cl) dissociative chemisorption is very high at 137.9 kJ/mol. In $Au_{10}Pd_{10}^-$ bimetallic cluster which simulates $Au_{0.5}Pd_{0.5}$ alloy, we found two types of intermediates for chemisorption. The adsorption was calculated to proceed with low activation energy barrier of 63.1 kJ/mol to give adsorption intermediate (Int_A2) in which both the phenyl group and the Cl atom are attached to the same Pd site. The other intermediate for dissociative chemisorption (Int_B2) is also stable as the adsorbed complex (Ads) or Int_A2. The calculated activation energy barrier from Int_A2 is 56.0 kJ/mol. The reaction pathway, which directly provides Int_B2 from the adsorption complex is also possible and has a moderate energy barrier of 52.6 kJ/mol. Note that an intermediate corresponding to Int_A2 was not obtained in the case of Au_{20}^- system. These results clearly show that the inclusion of Pd has an effect of stabilizing the dissociative adsorption and reducing activation energy, which is not possible in pure Au cluster.

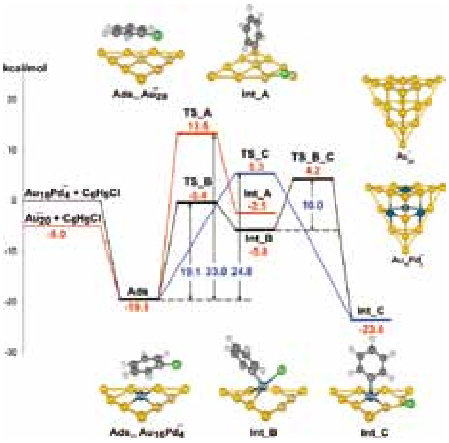

Figure 2. Energy profile diagram of oxidative addition of chlorobenzene on Au_{20}^- and $Au_{10}Pd_{10}^-$ NCs.

References

1) S. Higashibayashi, S. Onogi, H. K. Srivastava, G. N. Sastry, Y.-T. Wu and H. Sakurai, *Angew. Chem., Int. Ed.* **52**, 7314–7316 (2013).
2) R. N. Dhital, C. Kamonsatikul, E. Somsook, K. Bobuatong, M. Ehara, S. Karanjit and H. Sakurai, *J. Am. Chem. Soc.* **134**, 20250–20253 (2012).

Awards

HIGASHIBAYASHI, Shuhei; Insentive Award in Synthetic Organic Chemistry (2012).
HIGASHIBAYASHI, Shuhei; Sumitomo Chemical Award in Synthetic Organic Chemistry (2012).
HAESUWANNAKIJ, Setsiri; Best Poster Presentation, PERCH-CIC Congress VIII (2013).